Proceedings of the IASTED International Conference
COMPUTATIONAL AND SYSTEMS BIOLOGY
November 13–14, 2006, Dallas, TX, USA
ISBN CD: 0-88986-601-5

UNBINDING SIMULATION OF KINESIN'S NECK LINKER

Wonmuk Hwang
Department of Biomedical Engineering
Texas A&M University
College Station, TX 77843, USA
email: hwm@tamu.edu

Matthew J. Lang
Department of Mechanical Engineering, Biological Engineering Division
Massachusetts Institute of Technology
Cambridge, MA 02139, USA
email: mjlang@mit.edu

Martin Karplus
Department of Chemistry and Chemical Biology
Harvard University, Cambridge, MA 02138, USA
and
Laboratoire de Chimie Biophysique, ISIS
Université Louis Pasteur
67000 Strasbourg, France
email: marci@tammy.harvard.edu

ABSTRACT

Kinesin's neck linker is known to play a critical role in its nucleotide-dependent motility. However, it remains unclear how the neck linker binds and unbinds on the kinesin motor head as it walks on the microtubule and generates a walking stroke. To elucidate the nature of the interaction between the neck linker and motor head, we performed molecular dynamics simulations in which the neck linker is pulled out of the binding pocket by external forces. We found that it unbinds in a stepwise manner, in which N334 located in the middle of the neck linker keeps it from complete unbinding, creating an intermediate state. The rest of the neck linker rapidly unbinds once N334 releases from the motor head. Furthermore, we found that the N-terminal *cover strand* forms a β-sheet with the base portion of the neck linker, which can potentially control kinesin motility by affecting its conformational behavior. Our characterization of subdomains in the neck linker and their binding partners will help elucidate the walking mechanism of kinesin.

KEY WORDS
kinesin, myosin, steered molecular dynamics, molecular motor, motor protein, motility

1 Introduction

Kinesin is a biped motor protein that walks along microtubule tracks in a cell and performs diverse tasks, including intracellular cargo transport and cell division [1]. To date, it is the smallest known processive motor protein. Understanding how it works as a mechanical amplifier that converts the chemical energy of adenosine triphosphate (ATP) into mechanical work is important for elucidating how molecular motors work, in general.

Structurally, a kinesin monomer is composed of a $\sim$340 residue N-terminal globular motor head that possesses ATPase and microtubule binding activities, a $\sim$485 residue α-helical stalk, and finally a $\sim$92 residue C-terminal light chain domain involved with cargo binding [2]. Experiments have shown that the 10-15 amino acid long *neck linker*, which connects the motor head and the α-helical stalk, plays a crucial role in kinesin motility [3, 4]. In the ATP-state, the neck linker is bound to the motor head, while in the adenosine diphosphate- (ADP-) or nucleotide free state, it is detached from the motor [5]. However, the detailed nature of the interaction between the neck linker and the binding pocket in the motor head is currently not known.

To address this issue, we used molecular dynamics (MD) simulation in which the neck linker is forced to unbind from the neck binding pocket by applying a pulling force on the neck helix. Our results indicate that the unbinding occurs in two steps, showing modularized interaction between the neck linker and the binding pocket. This conclusion is of interest for further investigations of the physical nature of substeps in kinesin motility [6, 7].

2 Methods

2.1 Setting up the molecule

For the simulations, we used a monomeric rat kinesin structure (PDB ID: 2KIN, 1.9 Å resolution). It is in an ATP-like state, so that the neck linker is bound to the motor head. In the structure, coordinates are missing for the L11 loop region (amino acid (AA) 240-251). It is one of the microtubule binding domains, and the coordinates are filled in by the ModLoop utility available on the web (http://alto.compbio.ucsf.edu/modloop//modloop.html) [8]. The constructed loop has a β-hairpin fold, but the precise conformation is not relevant to the calculations since the loop is located far from the neck binding pocket

and no allosteric effect of L11 to the unbinding of the neck linker was observed.

2.2 Steered Molecular Dynamics (SMD)

All MD simulations were performed using CHARMM [9] with the param22 all-atom force field. To incorporate solvation effects into the simulation, the GBMV II continuum solvent model in CHARMM was used [10]. Pulling simulations of the neck helix was performed in the following way.

Atoms pulled. Twelve C_α atoms of the helix were pulled (AA 340-351, spheres in Fig. 1). Either 10 pN or 40 pN per atom was applied, totaling 120 pN or 480 pN. Two pulling directions were tested, marked 'Dir 1' and 'Dir 2' in Fig. 1. Dir 1 is in the direction along the helical axis, which was calculated using the COOR HELIX command in CHARMM. Dir 2 is perpendicular to the β10 strand at the base of the helix (defined in Fig. 3a), and points in between the C_α atoms of M1 and K160. More specifically, let $\hat{u}_2$: unit vector denoting Dir 2, $\hat{u}_{10}$: unit vector along the direction of β10, $\vec{r}_M$: position vector of M1 C_α, $\vec{r}_K$: position vector of K160 C_α, and $\vec{r}_B$: position vector of the base of the pulled helix. We then define

$$\vec{r} = \frac{\vec{r}_M + \vec{r}_K}{2} - \vec{r}_B \tag{1}$$

as the vector pointing from the base of the pulled helix to the midpoint between C_α's of M1 and K160. Then Dir 2 is

$$\hat{u}_2 = \vec{r} - (\vec{r} \cdot \hat{u}_{10})\hat{u}_{10}. \tag{2}$$

The shaded triangle in Fig. 1 is a visual guide for Dir 2.

Fixed atoms. To hold the motor head in place, C_α atoms of the putative microtubule binding domains (except L11) were harmonically constrained with a force constant of 10.0 kcal/(mol·Å^2). Fig. 1a is a view from the microtubule (bottom view), while Fig. 1b is a view from the plus end of the microtubule.

Molecular Dynamics. After initial minimization to remove bad contacts, the system was heated from 98 K to 300 K in 3 ps by Nosé-Hoover dynamics [11]. After heating, constraints on the microtubule binding domain and the pulling force were applied, and the production run was carried out for 400 ps with a 2 fs integration time step. Atomic coordinates were saved every 1 ps.

3 Results

Unbinding of the neck linker was not observed with a pulling force of 120 pN, while pulling with 480 pN resulted in unbinding within 400 ps of simulation (Fig. 2). No further unfolding of the protein occurred after the neck linker detached, suggesting that the core of the motor domain is stably folded. While a prolonged simulation time would eventually lead to unfolding of the motor head core, such a regime would be irrelevant to the experimental situation

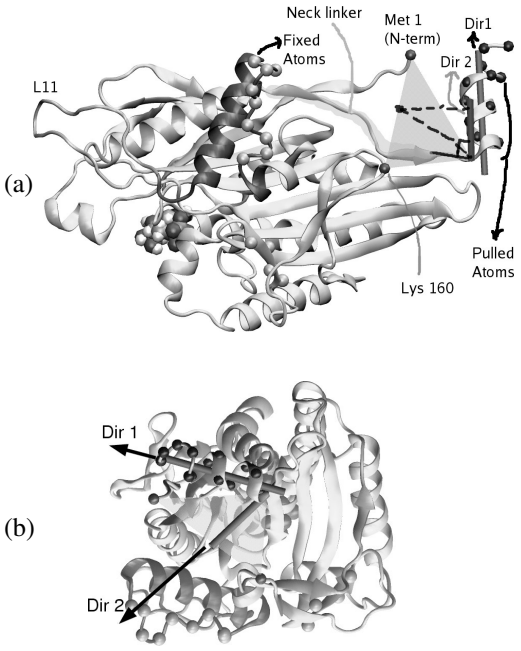

Figure 1. Simulation setup. (a) View from microtubule binding domains. (b) View from the plus end of the microtubule. Dir 1 & 2 are shown as cylindrical rods and arrows. In this view, a bound microtubule would be located below the molecule, approximately perpendicular to the page.

in which kinesin functions as a folded unit. Analysis of the unbinding trajectory revealed the following features:

(1) Unbinding occurs in a stepwise manner. Fig. 2 shows the center of mass distance trajectory of the pulled helix from its original position. In the graph, β10 is the C-terminal half of the neck linker (AA 335-338) that quickly unbinds after the pulling force is applied (Fig. 3a). After this initial partial unbinding, the system spends some time before zipper-like unbinding of the rest. During the intermediate stage, N334 located between β9 (AA 325-333) and β10 prevents the zipper-like unbinding of β9. Such behavior was observed in both simulations whether the neck helix was pulled in Dir 1 or Dir 2. Interestingly, N334 is highly conserved among different species [3].

(2) Surprisingly, in both simulations the N-terminal strand (AA 1-9) followed the neck linker as it moved away from the motor head. In the neck-bound structure, the strand forms a β-sheet with the β9 portion of the neck linker, in a conformation that covers β9. Hence we term it the *cover-strand*. The β-sheet remained intact even after complete unbinding (Fig. 3b). We found that this β-sheet is present in other structures of the kinesin family in the neck-bound state, which include conventional kinesin (3KIN: dimer structure of 2KIN, 1MKJ: human), Kif1A (1I6I: mouse, 1VFV: human), and Kif11 (1Q0B: human). However, this motif is absent in structures in which the neck linker is unbound. This suggests that the cover-neck β-sheet forms or

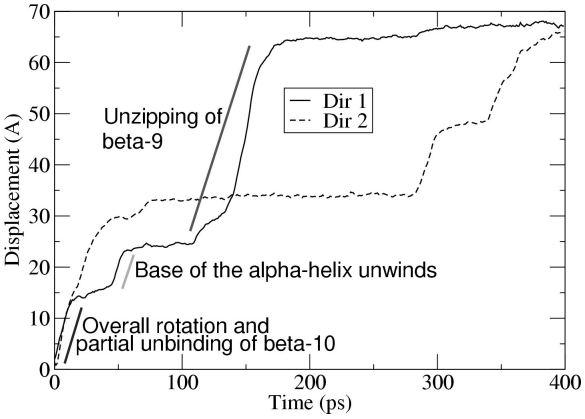

Figure 2. Center of mass displacement of the pulled helix. The unwound portion of the neck α-helix is shown in Fig. 3.

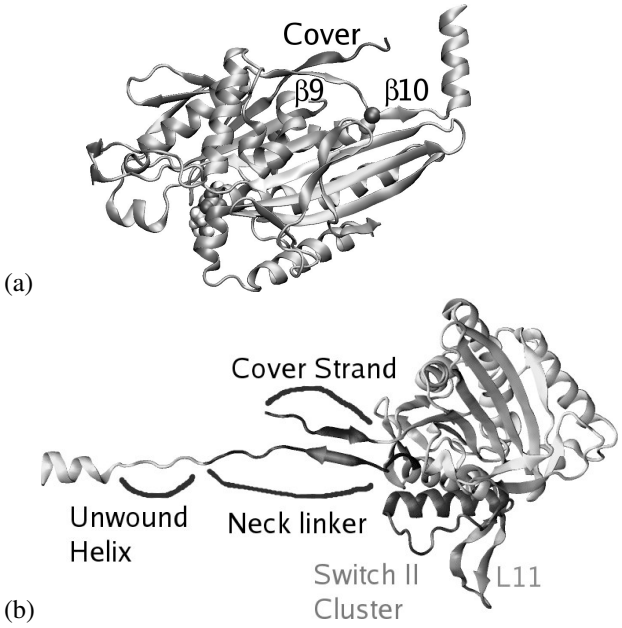

Figure 3. (a) Nomenclature for the subdomains of the neck linker [12] and the cover strand. N334 (dark sphere) is located between β9 and β10. (b) Final configuration of the Dir 1 simulation with a pulling force of 480 pN. View from a direction similar to Fig. 1b.

breaks depending on the nucleotide state, which can potentially control kinesin's walking stroke.

(3) In the case of Dir 1, we observed that ADP detaches after complete unzipping of the neck linker (data not shown). More careful analysis is required to address the order in which the neck linker unbinding and ADP release occur in the mechanochemical cycle of kinesin.

4 Concluding Discussion

To date, the role of the N-terminal cover strand has not been considered in kinesin motility. Our results suggest that the concerted motion of the neck linker and the cover strand could impose a directional constraint on the walking motion of the motor head, as compared to the case with the isolated neck linker. In Fig. 3b, the base of the neck linker can easily bend in and out of the page (along the microtubule), but bending in the plane of the page (transverse direction) is suppressed because of the presence of the cover strand. Such considerations could play a role in interpreting force clamp experiments where directional anisotropy in kinesin motility has been found [6]. Our result is not likely to be dependent on microtubule binding. As can be seen in Fig. 3b, the cover strand is distant from the microtubule, whereas microtubule binding domains switch II and L11 directly interact with it upon binding. Thus the concerted motion of the cover strand and the neck linker would not be affected by the presence of the microtubule.

Published discussions emphasize the control of the neck linker by the switch II cluster (Fig. 3b). For example, two conformations of switch II have been observed using a combination of x-ray crystallography and electron paramagnetic resonance (EPR) spectroscopy, called 'obstructive' (ADP or nucleotide-free) and 'unobstructive' (ATP state) [13]. By comparing the ADP and ATP-like structures of Kif1A with a bound and unbound neck linker, Kikkawa and co-workers [14] used the expression 'the neck linker melts away' depending on the conformation of the switch II cluster. However, as the simulation shows, switch II, located at the base of the neck liner, does not play any direct role in the initial unbinding of the neck linker. It is also far from the critical N334, whose release results in the zipper-like unbinding. N334, on the other hand, interacts with the the core of the motor domain, which is rigid (Figs. 4 & 5). Thus it is unlikely to bind or unbind directly by the conformational change of the switch II cluster alone.

It has been observed that the motor domain rotates by 20 degrees on the microtubule depending on the nucleotide state [14]. This is presumably caused by a conformational change of switch II (bound to microtubule) in the trailing head. Rotation of the motor domain relative to the neck linker that is held stationary by the coiled-coil stalk, may cause it to unbind. On the other hand, when the neck linker rebinds to the motor domain, switch II could play a more direct role, since it is located close to the N terminal end of the neck linker, where the reverse zipper-like binding initiates.

In summary, our simulation revealed substructures within the neck linker; they are β9, N334, and β10. β9 forms a β-sheet with the N-terminal cover strand in the neck-bound state. Since this secondary structure is absent in kinesin structures with an unbound neck linker, differential formation of the cover-neck bundle might play a role in kinesin motility. N334 operates as a latch that holds the neck linker once it zippered to the binding pocket. Finally, β10 forms a weak β-sheet with kinesin's motor head, com-

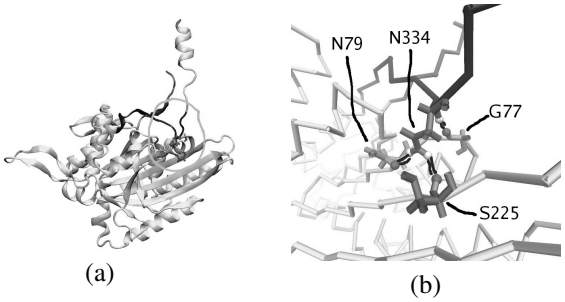

Figure 4. (a) Intermediate conformation at 100 ps point during the Dir 1 simulation. (b) Magnified view of the circle in (a), viewed from the right in (a). The interaction pairs are denoted by thick double lines: N334 HN - G77 O, N334 HD21 - S225 O, N334 HD22 - N79 OD1.

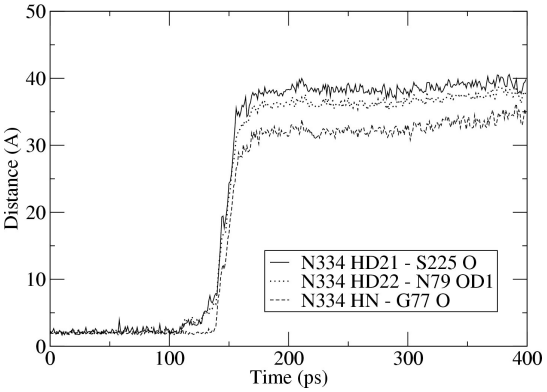

Figure 5. Distance between N334 with its interaction pairs in the Dir 1 simulation. Sharp transition from bound to unbound state shows that there is no further strong binding between the neck linker and the motor head after N334 is released.

pleting the zipper action of the neck linker. Further investigations are under way to clarify the mechanism by which these elements function cooperatively to generate a walking stroke.

References

[1] M. Schliwa, ed., *Molecualr Motors*. (ISBN:-527-30594-7: Wiley-VCH, 2003).

[2] F. J. Kull, E. P. Sablin, R. Lau, R. J. Fletterick, and R. D. Vale, "Crystal structure of the kinesin motor domain reveals a structural similarity to myosin," *Nature*, vol. 380, 1996, 550–555.

[3] R. H. Wade and F. Kozielski, "Structural links to kinesin directionality and movement," *Nat. Struct. Biol.*, vol. 7, 2000, 456–460.

[4] S. Rice, Y. Cui, C. Sindelar, N. Naber, M. Matuska, R. Vale, and R. Cooke, "Thermodynamic properties of the kinesin neck-region docking to the catalytic core," *Biophys. J.*, vol. 84, 2003, 1844–1854.

[5] S. Rice, A. W. Lin, D. Safer, C. L. Hart, N. Naberk, B. O. Carragher, S. M. Cain, E. Pechatnikova, E. M. Wilson-Kubalek, M. Whittaker, E. Pate, R. Cookek, E. W. Taylor, R. A. Milligan, , and R. D. Vale, "A structural change in the kinesin motor protein that drives motility," *Nature*, vol. 402, 1999, 778–784.

[6] S. M. Block, C. L. Asbury, J. W. Shaevitz, and M. J. Lang, "Probing the kinesin reaction cycle with a 2d optical force clamp," *Proc. Natl. Acad. Sci. USA*, vol. 100, 2003, 2351–2356.

[7] M. E. Fisher and Y. C. Kim, "Kinesin crouches to sprint but resists pushing," *Proc. Natl. Acad. Sci. USA*, vol. 102, 2005, 16209–16214.

[8] A. F. A, R. K. Do, and A. Sali, "Modeling of loops in protein structures," *Protein Sci.*, vol. 9, 2000, 1753–1773.

[9] B. R. Brooks, R. E. Bruccoleri, B. D. Olafson, D. J. States, S. Swaminathan, and M. Karplus, "CHARMM: A program for macromolecular energy, minimization, and dynamics calculations," *J. Comp. Chem*, vol. 4, 1983, 187–217.

[10] M. S. Lee, F. R. Salsbury, Jr, and C. L. Brooks III, "Novel generalized born methods," *J. Chem. Phys.*, vol. 116, 2002, 10606–10614.

[11] W. G. Hoover, "Canonical dynamics: Equilibrium phase-space distributions.," *Phys. Rev. A*, vol. 31, 1985, 1695–1697.

[12] S. Sack, J. Müller, A. Marx, M. Thormählen, E.-M. Mandelkow, S. T. Brady, and E. Mandelkow, "X-ray structure of motor and neck domains from rat brain kinesin," *Biochem.*, vol. 36, 1997, 16155–16165.

[13] C. V. Sindelar, M. J. Budny, S. Rice, N. Naber, R. Fletterick, and R. Cooke, "Two conformations in the human kinesin power stroke defined by x-ray crystallography and EPR spectroscopy," *Nat. Struct. Biol.*, vol. 9, 2002, 844–848.

[14] M. Kikkawa, E. P. Sablin, Y. Okada, H. Yajima, R. J. Fletterick, and N. Hirokawa, "Switch-based mechanism of kinesin motors," *Nature*, vol. 411, 2001, 439–445.